11th International Conference on Emerging Nuclear Energy Systems (ICENES 2002) (September 29 - October 4, 2002, Albuquerque, NM)

The Cold Fusion Phenomenon and Its Application to Energy Production and Nuclear Waste Remediation

H. Kozima,
Physics Department, Portland State University
Portland, OR 97207-0751, USA
E-mail, cf-lab.kozima@pdx.edu
Website, http://web.pdx.edu/ pdx00210/

I would like to express my gratitude to the organizing committee for inviting me and others in my field to participate in this Conference on Emerging Nuclear Energy Systems. Our approach is different but the goalis the same. We all want to develop a new, clean energy sources.

First of all, it should be noticed that the cold fusion phenomenon (CFP) is a name for "nuclear reactions and accompanying events occurring in solids with high densities of hydrogen isotopes in ambient radiation."

The Cold Fusion Phenomenon as a New Field of Solid State-Nuclear Physics is applicable to Radioactivity and Energy Problems.

Present Quantum Mechanics is applicable to this field.

This presentation consists of following sections.

1. Short History of Cold Fusion Phenomenon (CFP)

1-1. Fleischmann, Pons, Hawkins

1-2. S.E. Jones et al.

1-3. DOE Report

1-4. An Episode - Reality of the d-d Fusion Reactions in Solids

It is advisable to recollect some episodes in the early days of CFP research to resolve some prejudice in our mind if any.

1-1. Fleischmann, Pons, Hawkins

(1) M. Fleischmann, S. Pons and M. Hawkins, "Electrochemically induced Nuclear Fusion of Deuterium", *J. Electroanal. Chem.* **261**, 301 (1989).

Table 1 of M. Fleischmann et al. Generation of excess enthalpy in Pd cathodes as a function of current density and electrode size.

TABLE 1

Generation of excess enthalpy in Pd cathodes as a function of current density and electrode size

Electrode type	Dimensions /cm	Current density /mA cm^{-2}	Excess rate of heating/W	Excess specific rate of heating/W cm^{-3}
Rods	0.1×10	8	0.0075	0.095
		64	0.079	1.01
		512 [a]	0.654 [a]	8.33
	0.2×10	8	0.036	0.115
		64	0.493	1.57
		512 [a]	3.02 [a]	9.61
	0.4×10	8	0.153	0.122
		64	1.751	1.39
		512 [a]	26.8 [a]	21.4
Sheet	0.2×8×8	0.8	0	0
		1.2	0.027	0.0021
		1.6	0.079	0.0061
Cube	1 ×1×1	125	WARNING! IGNITION? See text	
		250		

[a] Measured on electrodes of length 1.25 cm and rescaled to 10 cm.

(2) S.E. Jones, E.P. Palmer, J.B. Czirr, D.L. Decker, G.L. Jensen, J.M. Thorne and S.E. Tayler, "Observation of Cold Nuclear Fusion in Condensed Matter", *Nature* **338**, 737 (1989).

Fig. 2 of S.E. Jones et al. Neutron Energy Spectrum.

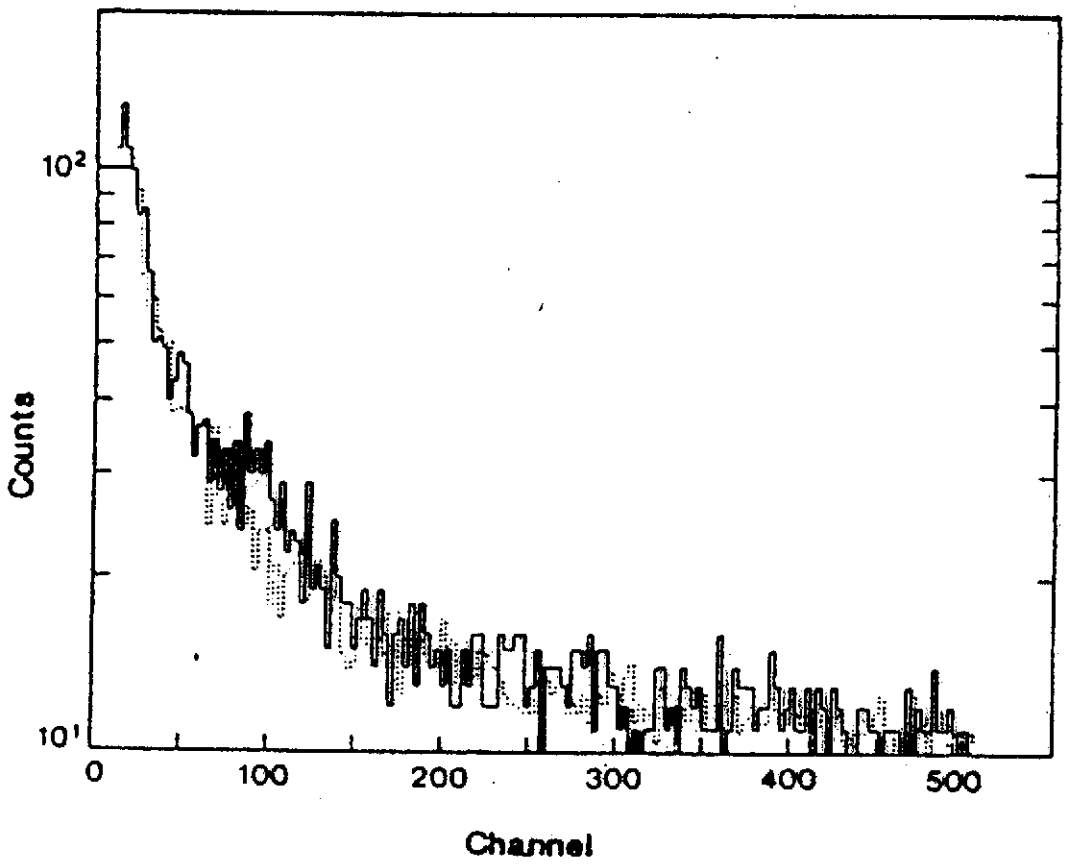

FIG. 2 Foreground (solid) and background (dashed) counts as a function of pulse height (corresponding to neutron energy) in the neutron spectrometer. Ten counts have been added to each three-channel bin for clarity of presentation.

NATURE · VOL 338 · 27 APRIL 1989

1-3. DOE Report

J. Huizenga, *Cold Fusion Research, November 1989–* A **Report of the Energy Research** Advisory Board to the United States Department of **Energy –** , DOE/S–0073, DE90, 005611.

This report sentenced "Death of CFP" based on inappropriate evidences and invalid conjectures.

1-4. An Episode - Reality of the *d-d* Fusion Reactions in Solids

J.R. Huizenga, *Cold Fusion – The Scientific Fiasco of the Century*, University of Rochester Press, Rochester, NY, USA, 1992.

Facts were discarded by an established framework.

H. Kozima, *Discovery of the Cold Fusion Phenomenon - Evolution of the, Solid State - Nuclear Physics and the Energy Crisis in 21st Century*, Ohtake Shuppan KK., Tokyo, Japan, 1998.

Theoretical effort to construct a framework to fit experimental facts.

Some data related with nuclear reactions between charged particles in solids.

$\varepsilon_d \sim 25$ meV

$\phi_{Coulombbarrier} \sim 10$ keV

$\lambda_{phonon}|_{min} \sim 1\ \mathring{A}$ $(\varepsilon_{phonon}|_{max} \sim 100$ meV)

$\lambda_{electron}|_{min} \sim \frac{h}{p}|_{max} \sim \frac{h}{p_F} \sim 98\ \mathring{A}$

($\varepsilon_e = 25$ meV, free electron $\varepsilon \sim$ kT)

$\lambda_{electron}|_{min} \sim \frac{h}{p}|_{max} \sim \frac{h}{p_F} \sim 2\ \mathring{A}$

($\varepsilon_e = 62.5$ eV, band electron at k $= \frac{\pi}{a}$)

$\lambda_{neutron} \sim \frac{h}{p}|$

$= 1\ \mathring{A}$ $(\varepsilon_n = 0.13$ eV)

$= 2.28\ \mathring{A}$ $(\varepsilon_n = 25$ meV)

2. Experimental Facts of CFP

2-1. Summary, Table 1

2-2. Characteristics of CFP

2-3. Data 1, Table 2

2-4. Data 2, Table 3

2-5. Data 3, Table 4

2-6. Data 4, Table 5

There are too many experimental data sets with various kinds of events from excess heat to nuclear transmutations of heavy elements to introduce in a paper as this one.

Our approach throughout this work is to consider these events in CFP have common cause even if it is possible to consider each event has different cause not related with others.

2-1. Summary, Table 1

"Discovery" Table 5.1 (revised).

Table 1: Matrix Substances, Agent nuclei, Direct and Indirect Evidences of nuclear reactions in cold fusion phenomenon (CFP). Q is for the excess heat and NT for the nuclear transmutation). Energy ε and position $\boldsymbol{r}$ dependences of products, decay time shortening of radioactive nuclides, and fission-barrier decrease of compound nuclides give direct information of nuclear reactions in CFP.

Matrix Substance	Agent	Direct Evidence	Indirect Evidence
Pd, Ti, Ni	${}^{2}_{1}\mathrm{H} \equiv d$	Gamma rays γ (ε)	Excess heat Q
KCl + LiCl	${}^{1}_{1}\mathrm{H} \equiv p$	Neutron energy spectra n (ε)	Neutrons n
$ReBa_2Cu_3O_7$	${}^{6}_{3}\mathrm{Li}$	Spatial distribution	Tritium ${}^{3}_{1}\mathrm{H} \equiv \mathrm{T}$
Na_xWO_3	${}^{10}_{5}\mathrm{B}$	of NT products $({}^{A'}_{Z'}\mathrm{M}(\boldsymbol{r}))$	Helium ${}^{4}_{2}\mathrm{He}$
KD_2PO_4	${}^{39}_{19}\mathrm{K}$	Decay time shortenings	NT (NT_D,NT_F,NT_A)
TGS	${}^{85}_{37}\mathrm{Rb}$,${}^{87}_{37}\mathrm{Rb}$	Fission-barrier decrease	X-ray $X(\varepsilon)$
$SrCe_aY_bNb_cO_d$	${}^{1}_{0}\mathrm{n} \equiv n$		

There are complicated experimental data sets showing various kinds of events in cold fusion phenomenon (CFP).

Materials where occluded hydrogen isotopes (protium and/or deutrium) are mainly transition metals but also others as listed in the first column.

Activation agents are some alkaline metal electrolytes in addition to hydrogen isotopes as listed in the second column.

There are two kinds of evidences, direct and indirect, for nuclear reactions in the above specified solids as complex systems as listed in the third and fourth columns, respectively.

Complexity revealed in this table show that CFP is a result of complicated processes occurring in complex system composed of elements listed in the first and second columns.

2-2. Characteristics of CFP

1. Products of CFP includes excess heat Q, ^{4}He, ^{3}H, other nuclides by nuclear transmutations (NT's), and others.
2. Occurrence of CFP in both protium and deuterium system in ambient radiation
3. Mainly in transition-metal hydrides and deuterides with appropriate electrolyte
4. Boundary layers of widths about a few micrometers are essential fields of reactions
5. Reactions occur sporadically and intermittently with the qualitative reproducibility
6. There are definite relations between amounts of products Q, N_{NT}, N_{He}, N_t, and others. $N_Q \equiv$ Q (MeV)/5 MeV.
7. Scarceness of neutrons and gammas compared with nuclear reactions in free space

Nuclear Reactions in Free Space vs. Nuclear Reactions in Solids

Therefore, the cold fusion phenomenon (CFP) should be interpreted as "nuclear reactions and accompanying events occurring in solids with high densities of hydrogen isotopes in ambient radiation."

2-3. Data 1, Table 2

Table 2: Results of TNCF Model Analyses explained in Section 4. (1) Pd/D(H)/Li System. Neutron Density n_n and Relations between the Numbers N_x of Event x Obtained by Theoretical Analysis of Experimental Data on TNCF Model ($N_Q \equiv Q$ (MeV)/5 (MeV)). Typical value of the surface vs. volume ratio $S/V(\mathrm{cm}^{-1})$ of the sample is tabulated, also. References in this table are those in the book.[5]

Data No.	Authors	System	S/V cm^{-1}	Measured Quantities	n_n cm^{-3}	Other Results (Remarks)
1	Fleischmann et al.[1]	Pd/D/Li	6 ~ 40	Q , t, n $N_t/N_n \sim 4\times 10^7$ $N_Q/N_t \sim 0.25$	$\sim 10^9$	(Q =10W/cm^3) $N_t/N_n \sim 10^6$ $N_Q/N_t = 1.0$
2	Morrey et al.[1-4]	Pd/D/Li	20	Q ,^{4}He ^{4}He in $\ell \leq 25\mu$ m	4.8×10^8	$N_Q/N_{He} \sim 5.4$ (If 3% ^{4}He in Pd)
3	Packham[43]	Pd/D/Li	40	t in solution	3.6×10^7	
4	Chien et al.[43']	Pd/D/Li	4	^{4}He in surf. layer and t , no ^{3}He	1.8×10^6	$N_t/N_{He} \sim 1$(If few % ^{4}He in Pd)
5	Roulette[1"']	Pd/D/Li	63	Q	$\sim 10^{12}$	
6	Storms[4]	Pd/D/Li	9	$t(1.8\times 10^2 \mathrm{Bq/m}\ell)$	2.2×10^7	(τ=250h)
7	Storms[4']	Pd/D/Li	22	Q (Q_{max}=7W)	5.5×10^{10}	(τ=120h)
8	Takahashi et al.[5']	Pd/D/Li	2.7	t, n $N_t/N_n \sim 6.7\times 10^4$	3×10^5	$N_t/N_n \sim$ 5.3×10^5
9	Miles et al.[18']	Pd/D/Li	5	Q , ^{4}He (N_Q/N_{He}=1$\sim$ 10)	$\sim 10^{10}$	$N_Q/N_{He} \sim 5$
10	Okamoto et al.[12']	Pd/D/Li	23	Q , NT_D $\ell_0 \sim 1\ \mu$ m	$\sim 10^{10}$	$N_Q/N_{NT} \sim 1.4$ (^{27}Al$\rightarrow^{28}$Si)
11	Oya[12-5]	Pd/D/Li	41	Q , γ spectrum	3.0×10^9	(with^{252}Cf)
12	Arata. et al.[14]	Pd/D/Li	7.5 $\times 10^4$	Q , ^{4}He ($10^{20} \sim 10^{21}$ cm^{-3}) $N_Q/N_{He} \sim 6$	$\sim 10^{12}$	(Assume t channeling in Pd wall)
13	McKubre[3]	Pd/D/Li	125	Q (& Formula)	$\sim 10^{10}$	Qualit.explan.
14	Passell[3"']	Pd/D/Li	400	NT_D	1.1×10^9	N_{NT}/N_Q=2

The experimental data in columns $2-5$ show variety of systems, samples and measured quantities where observed positive results of CFP.

2-4. Data 2, Table 3

Table 3: Results of TNCF Model Analyses explained in Section 4. (1) Pd/D(H)/Li System (continued).

Data No.	Authors	System	S/V cm^{-1}	Measured Quantities	n_n cm^{-3}	Other Results (Remarks)
15	Cravens[24"]	Pd/H/Li	4000	Q (Q_{out}/Q_{in}=3.8)	8.5×10^9	(If PdD exists)
16	Bockris[43]	Pd/D/Li	5.3	t,^{4}He;$N_t/N_{He}\sim$ 240	3.2×10^6	$N_t/N_{He}\sim$ 8
17	Lipson[15-4]	Pd/D/Na	200	γ (E_γ=6.25MeV)	4×10^5	If effic. =1%
18	Will[45]	Pd/D_2SO_4	21	$t(1.8\times 10^5/cm^2s)$	3.5×10^7	(If $\ell_0\sim 10\mu$ m)
19	Cellucci et al.[51"']	Pd/D/Li	40	Q , ^{4}He N_Q/N_{He}=1$\sim$ 5	2.2×10^9	(IfQ =5W) N_Q/N_{He}=1
20	Celani[32"']	Pd/D/Li	400	Q (Q_{max}=7 W)	1.0×10^{12}	(If200%output)
21	Ota[53]	Pd/D/Li	10	Q (113%)	3.5×10^{10}	(τ=220 h)
22	Gozzi[51"]	Pd/D/Li	14	Q , t, ^{4}He	$\sim 10^{11}$	($\tau\sim 10^3$h)
23	Bush[27']	Ag/PdD/Li	2000	Q (Q_{max}=6W)	1.1×10^9	(τ=54d,Film)
24	Mizuno[26-4]	Pd/D/Li (If Cr in Pd)	3.4	Q , NT_D $\ell\leq 2\ \mu$ m)	2.6×10^8	τ=30d,Pd 1cm$\phi\times$ 10cm
25	Iwamura[17]	PdD_x	20	n (400/s),t	3.9×10^8	$4.4\times 10^6 t$/s
26	Itoh[17']	PdD_x	13.3	n (22/m),t	8.7×10^7	$7.3\times 10^{10} t$/s
27	Itoh[17"]	PdD_x	13.3	n (2.1×10^3/s)	3.9×10^8	
28	Iwamura[17"']	PdD_x	20	Q (4 W) NT_F(Ti, Cr etc.)	3.3×10^{10}	(NT_F? unexplained)
29	Milcy[65]	Pd/H/Li	150	NT_F(Ni, Zn,$\cdots$)	4.5×10^{12}	
30	Dash[59]	Pd/D,H_2SO_4	57	Q , NT_D	$\sim 10^{12}$	Pt$\rightarrow$Au
31	Szpak et al.[79-9]	Pd/D/Li	10^3(?)	t	$\sim 10^2$	Electroplated Pd
32	Clarke et al.[80']	Pd/D/Li	0.26(?)	(Q), t	$\sim 10^{10}$	Pd black[14]
33	Kozima[203]	Pd/D,H/Li	200	n (2.5×10^{-4}/s)	2.5×10^2	Effic. =0.44%

The experimental data in columns $2-5$ show variety of systems, samples and measured quantities where observed positive results of CFP.

2-5. Data 3, Table 4

Table 4: Results of TNCF Model Analyses explained in Section 4. (2) Ni/H/K System and Others. Explanation of this table is common to Table 2.

Data No.	Authors	System	S/V cm^{-1}	Measured Quantities	n_n cm^{-3}	Other Results (Remarks)
34	Jones[2]	Ti/D/Li	8.1	n (2.45 MeV)	3.1×10^{11}	
35	Mills[25]	Ni/H/K	160	Q (0.13 W)	3.4×10^{10}	
36	Bush[27']	Ni/H/K Ni/H/Na	~ 160 ~ 160	NT_D(Ca) NT_D(Mg)	5.3×10^{10} 5.3×10^{11}	$N_Q/N_{NT}\sim 3.5$ if τ=0 for ^{40}K)
37	Bush[27"]	Ni/H/Rb	$\sim 10^4$	NT_D(Sr)	1.6×10^7	$N_Q/N_{NT}\sim 3$
38	Savvatimova et al.[34"]	Pd/D_2	100	NT_D(Ag)	9×10^{10}	
39	Bockris et al.[43-6]	Pd/H/		NT_F(Mg,Si,Cs,Fe, etc. in 1μ m layer)	3.0×10^{11}	Only Fe(10%of Pd) is taken up.
40	Alekseev[44']	Mo/D_2	4.1	t ($\sim 10^7$/s)	1.8×10^7	(If MoD)
41	Romodanov et al.[44"']	TiC/D	4.1	t ($\sim 10^6$/s)	$\sim 10^6$	(D/Ti$\sim$ 0.5assumed)
42	Reifensch-weiler[38']	$TiT_{0.0035}$	7×10^5	β decay reduction	1.1×10^9	(T=0$\sim$ 450°C)
43	Dufour[7]	Pd, SS/D_2 Pd, SS/H_2	48	Q , t, n	9.2×10^{11} 4.0×10^9	(D(H)/Pd$\sim$ 1 is assumed)
44	Claytor[9]	Pd/D_2	400	t (12.5 nCi/h)	1.6×10^{13}	(If D/Pd$\sim$ 0.5)
45	Srinivasan[16]	Ti/D_2	1500	t ($t/d\sim 10^{-5}$)	1.9×10^8	(Aged plate)
46	De Ninno[6']	Ti/D_2	440	n , t	1.2×10^6	(D/Ti=1,1w)

The experimental data in columns $2-5$ show variety of systems, samples and measured quantities where observed positive results of CFP.

2-6. Data 4, Table 5

Table 5: Results of TNCF Model Analyses explained in Section 4. (2) Ni/H/K System and Others (continued). Δ(x) in this table means a change in the quantity x in the experiment.

Data No.	Authors	System	S/V cm^{-1}	Measured Quantities	n_n cm^{-3}	Other Results (Remarks)
47	Focardi[23]	Ni/H_2	8.2	Q	3.0×10^{12}	(IfN_p=10^{21})
48	Oriani[52]	$SrCeO_3/D_2$	22	$Q\sim 0.7$W	4.0×10^{10}	V=0.31cm^3
49	Notoya[35"]	Ni/D,H/K	3.4 $\times 10^4$	Q (0.9 W), t	2.4×10^{13}	(If a half of T is in liquid)
50	Notoya[35-4]	Ni/D,H/K	same	NT_D(Ca)	1.4×10^9	(Sintered Ni)
51	Yamada[54]	Pd/D_2	185	n , NT_D(C)	2.0×10^{12}	
52	Cuevas[55]	$TiD_{1.5}$	134	n (102 n/s)	5.4×10^{11}	
53	Niedra[56]	Ni/H/K	80	Q (4 W)	1.4×10^9	5km$\times$ 0.5mmϕ
54	Ohmori[22"]	Au/H/K	200	Q , NT_F(Fe)	$\sim 10^{11}$	(Au plate)
55	Li[57]	Pd/D_2	185	Q	1.6×10^{12}	(Pd wire)
56	Qiao[57']	Pd/H_2	185	NT_F(Zn)	3.8×10^{10}	(40%NTin 1y)
57	Bressani[58']	Ti/D_2	$\leq 10^3$?	n (ε)	10^4– 10^7	(Ti shaving)
58	Miley[65']	Ni/H/Li	50	NT_D(Fe, Cr,$\cdots$)	1.7×10^{12}	
59	Botta[58"]	Pd/D_2	$\leq 10^3$?	^{4}He	7×10^{12}	(0.1 mm Pd sheet)
60	Coupland et al[81]	Pd/H,D	~ 4	$\Delta(^7Li/^6Li)$=60-90% if $(^7Li/^6Li)_0$=12.5	3.5-4.1$\times 10^8$	Pd rod returned by F. and P.[1]
61	Passell[3-6]	Pd/H_2	185(?)	$\Delta(^7Li/^6Li)$=100%	4.4×10^8	Pd wire[57-3]

The experimental data in columns $2-5$ show variety of systems, samples and measured quantities where observed positive results of CFP.

3. Theoretical Efforts based on Quantum Mechanics – What is the missing factor of CFP?

3-1. *d-d* Fusion Reactions in Free Space

3-2. Denial of *d-d* Fusion Reactions in Solids

3-3. Brief Understanding of *d-d* Fusion Reactions in Solids

3-4. TNCF Model Explanation of CFP

When there is a new phenomenon, it should be caused by a new unknown mechanism in the known components or by a new component not noticed before. Those elements causing the new phenomenon are missing factors. What is then the missing factor or factors of CFP.

From my point of view, it is in the known physics of solids and nuclei based on quantum mechanics. One possibility is physics of low energy neutrons in solids which has not well known until now and also low lying neutron levels in heavy nuclei as elaborated in this presentation.

3-1. *d-d* Fusion Reactions in Free Space

d-d fusion reactions in free space (and their branching ratios)

$$\begin{aligned} d + d &= {}^{3}_{2}\mathrm{He}\,(0.82\ \mathrm{MeV}) + n\,(2.45\ \mathrm{MeV}), \quad (1) \\ &= t\,(1.01\ \mathrm{MeV}) + p\,(3.02\ \mathrm{MeV}), \quad (1) \\ &= {}^{4}_{2}\mathrm{He}\,(76.0\ \mathrm{keV}) + \gamma\,(23.8\ \mathrm{MeV}), \quad (10^{-6}) \end{aligned}$$

Those reactions observed in free space are difficult to occur in solids without special acceleration mechanisms. In addition to this fact, the branching ratios of the nuclear products observed in CFP are in contraction with experimental data.

3-2. Denial of *d-d* Fusion Reactions in Solids

A.J. Leggett and G. Baym, "Exact Upper Bound on Barrier Penetration Probabilities in Many-Body Systems: Application to 'Cold Fusion'", *Phys. Rev. Letters* **63**, 191 (1989).

S. Ichimaru, "Nuclear Fusion in Dense Plasmas", *Rev. Mod. Phys.* **65**, 255 (1993).

Occurrence of *d-d* fusions in solids are theoretically denied by many physicists including those listed above. To insist the occurrence of *d-d* fusion in solids, it is absolutely demanded to surmount discussions given in these papers.

3-3. Brief Understanding of Characteristics of *d-d* Fusion Reactions in Solids

The deuteron - deuteron interaction in solids is essentially the same that in free space due to the following facts.

Effective length of the nuclear force of order 1 fm is too short (five orders of magnitude short) to be influenced by phonons of minimum wave length of about 1 0^5 fm and by electrons of minimum wave length of about 10^3 fm.

Electromagnetic wave with a wave length of 1 fm has an energy of about 10^9 eV.

Brief Explanation of Difficulty to Induce Characteristic Reaction in CF Matter

Figurative Explanation

$$\Phi_{Coulomb\ barrier} \sim 10 \text{ keV}$$
$$\lambda_{phonon}|_{min} \sim a_{lattice} \sim 1\ \mathring{A}, \quad (\varepsilon_{max} \sim 100 \text{ meV}).$$

$$\lambda_{electron}|_{min} \sim \frac{h}{p_{max}} \sim \frac{h}{p_F} \sim 98\ \mathring{A}\ \ (\varepsilon_e = 25 \text{ meV}),$$
$$\sim 2\ \mathring{A}\ \ (\varepsilon_e = 62.5 \text{ eV at } k = \pi/a),$$

$$\lambda_{neutron} = \frac{h}{p} = 1\ \mathring{A},\ \ (\varepsilon_n = 0.13 \text{ eV}),$$
$$= 2.28\ \mathring{A},\ \ (\varepsilon_n = 25 \text{ meV}).$$

3-3. Brief Understanding of Characteristics of d-d Fusion Reactions in Solids

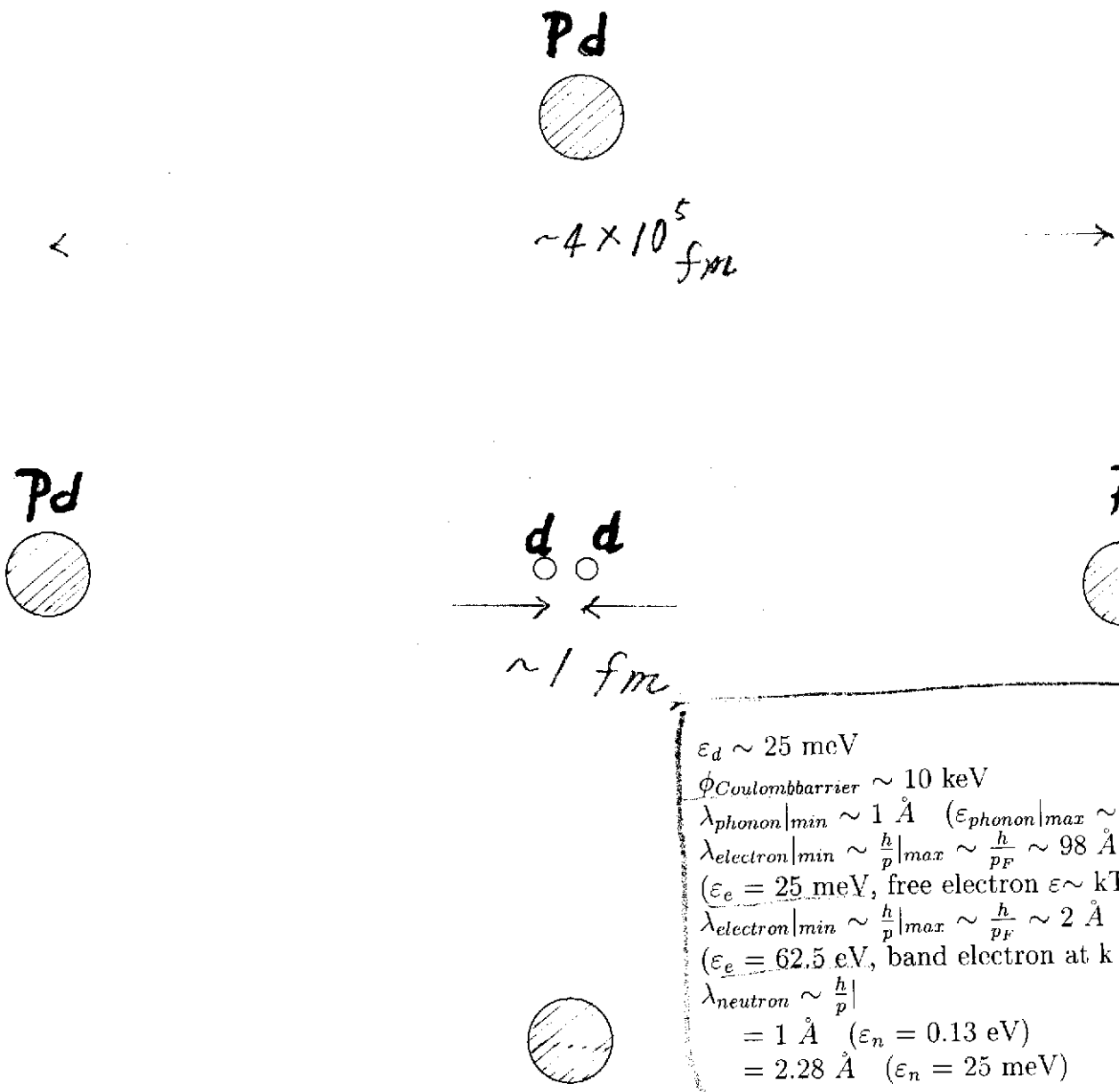

$\varepsilon_d \sim 25$ meV

$\phi_{Coulombbarrier} \sim 10$ keV

$\lambda_{phonon}|_{min} \sim 1$ Å $\quad (\varepsilon_{phonon}|_{max} \sim 100$ meV)

$\lambda_{electron}|_{min} \sim \frac{h}{p}|_{max} \sim \frac{h}{p_F} \sim 98$ Å

($\varepsilon_e = 25$ meV, free electron $\varepsilon \sim$ kT)

$\lambda_{electron}|_{min} \sim \frac{h}{p}|_{max} \sim \frac{h}{p_F} \sim 2$ Å

($\varepsilon_e = 62.5$ eV, band electron at k = $\frac{\pi}{a}$)

$\lambda_{neutron} \sim \frac{h}{p}|$

$= 1$ Å $\quad (\varepsilon_n = 0.13$ eV)

$= 2.28$ Å $\quad (\varepsilon_n = 25$ meV)

3-4. TNCF Model Explanation of CFP

Phenomenological Approach to CFP using Experimental Facts as Supports (Premises)

Premise 1. We assume a priori existence of the quasi-stable trapped neutron with a density n_n in pertinent solids, to which the neutron is supplied essentially from the ambient neutron at first and then by breeding processes (explained below) in the sample. (Null Results without bg. neutrons $\rightarrow n_n$.)

The density n_n is a single adjustable parameter in this model. other premises are common for all materials and situations.

Premise 2. The trapped neutron in a solid reacts with another nucleus in the surface layer of the solid, where it suffers a strong perturbation, as if they are in vacuum. We express this property by taking the parameter (the instability parameter) ξ, defined in the relation (2) written down below, as $\xi = 1$. (Local production of nuclear products $\rightarrow \xi = 1$.)

Premise 3. The trapped neutron reacts with another perturbing nucleus in volume by a reaction rate given in the relation (2) below with a value of the instability parameter $\xi \leq 0.01$ due to its stability in the volume (except in special situations such as at very high temperature as 3000 K). (Some evidence of nuclear reaction in volume $\rightarrow \xi \leq 0.01$.)

4. Analysis of Experimental Data Sets by the TNCF Model

The same nuclear reactions in the free space are used in the analysis of CFP which occurs in solids assuming the trapped thermal neutrons behave as free particles in solids.

4-1. Reactions used in the TNCF Model (1)

(1) Trigger reactions.

Trigger reactions are induced by trapped neutrons feeded from ambient thermal neutrons. Gamma rays emitted in reactions in free space are supposed to be dissipated by other channels present in solids that will be explained in Section 5.

$$n + {}^{A}_{Z}\mathrm{M} = {}^{A+1-b}_{Z-a}\mathrm{M}' + {}^{b}_{a}\mathrm{M}'' + Q,$$

$$n + {}^{6}_{3}\mathrm{Li} = {}^{4}_{2}\mathrm{He}\ (2.1\ \mathrm{MeV}) + t\ (2.7\ \mathrm{MeV}).$$

$$\begin{aligned} n + d &= t\ (6.98\ \mathrm{keV}) + \gamma\ (6.25\ \mathrm{MeV}), \\ n + {}^{7}_{3}\mathrm{Li} &= {}^{8}_{3}\mathrm{Li} = {}^{8}_{4}\mathrm{Be} + e^{-} + \bar{\nu}_e + 13\ \mathrm{MeV}, \\ {}^{8}_{4}\mathrm{Be} &= 2\ {}^{4}_{2}\mathrm{He} + 3.2\ \mathrm{MeV}. \end{aligned}$$

$$n + p = d\ (1.33\ \mathrm{keV}) + \gamma\ (2.22\ \mathrm{MeV}).$$

4-2. Reactions used in the TNCF Model (2)

(2) Breeding reactions.

Breeding reactions are induced by trapped neutrons feeded from ambient thermal neutrons and also by trigger reactions explained above. Gamma rays emitted in reactions in free space are supposed to be dissipated by other channels present in solids that will be explained in Section 5.

$$t\ (\varepsilon) + d\ =\ {}^{4}_{2}\mathrm{He}\ (3.5\ \mathrm{MeV}) + n\ (14.1\ \mathrm{MeV}).$$

$$\begin{aligned} n\ (\varepsilon) + d &= n'\ (\varepsilon') + d'\ (\varepsilon''), \\ n\ (\varepsilon) + d &= n' + p + n'', \\ n\ (\varepsilon) + {}^{A}_{Z}\mathrm{M} &= {}^{A-1}_{Z}\mathrm{M} + n + n', \\ n\ (\varepsilon) + {}^{A}_{Z}\mathrm{M} &= {}^{A-A'+1}_{Z-Z'}\mathrm{M}' + {}^{A'}_{Z'}\mathrm{M}''. \end{aligned}$$

$$\begin{aligned} d\ (\varepsilon) + d &= t\ (1.01\ \mathrm{MeV}) + p\ (3.02\ \mathrm{MeV}), \\ &= {}^{3}_{2}\mathrm{He}\ (0.82\ \mathrm{MeV}) + n\ (2.45\ \mathrm{MeV}), \end{aligned}$$

4-3. Relations between N_x's in TNCF Model

The TNCF model gives numerical relations between products of CFP which can be compared with experimental results obtained in experimental data sets listed in following tables 2 - 5.

$$N_t\ =\ N_{He}\ =\ N_Q\ \equiv\ Q\ (\mathrm{MeV})/4.8\ (\mathrm{MeV}). \tag{1}$$

$$N_t\ =\ N_{He} \tag{2}$$

$$N_n/N_t\ =\ 9.5 \times 10^{-7}\ \sim\ 10^{-6}. \tag{3}$$

4-4. Analysis 1, Table 2

Columns 6 and 7 of Table 2 in Section 2.

4-5. Analysis 2, Table 3

Columns 6 and 7 of Table 3 in Section 2.

4-6. Analysis 3, Table 4

Columns 6 and 7 of Table 4 in Section 2.

4-7. Analysis 4, Table 5

Columns 6 and 7 of Table 5 in Section 2.

5. Quantum Mechanical Verification of Premises in the TNCF Model

5-1. Neutron Conduction Bands

5-2. Neutron Valence Bands

5-3. Local Coherence of Neutron Bloch Waves at Boundary

5-4. Neutron Drops - Clusters of $(A\text{-}Z)$ Neutrons and (Z) Protons

5-5. Analogy with Neutron Star Matter

It should be emphasized that the physics of particles in an energy range up to several hundred MeV is well discribed by present quantum mechanics even if it is possible to innovate quantum mechanics fundamentally to treat some phenomena introducing new elements not noticed before. However, I think CFP is not the case and can be treated by quantum mechanics as far as I know the data obtained there.

5-1. Neutron Conduction Bands

H. Kozima, "Neutron Band in Solids", *J. Phys. Soc. Japan* **67**, 3310 (1998).

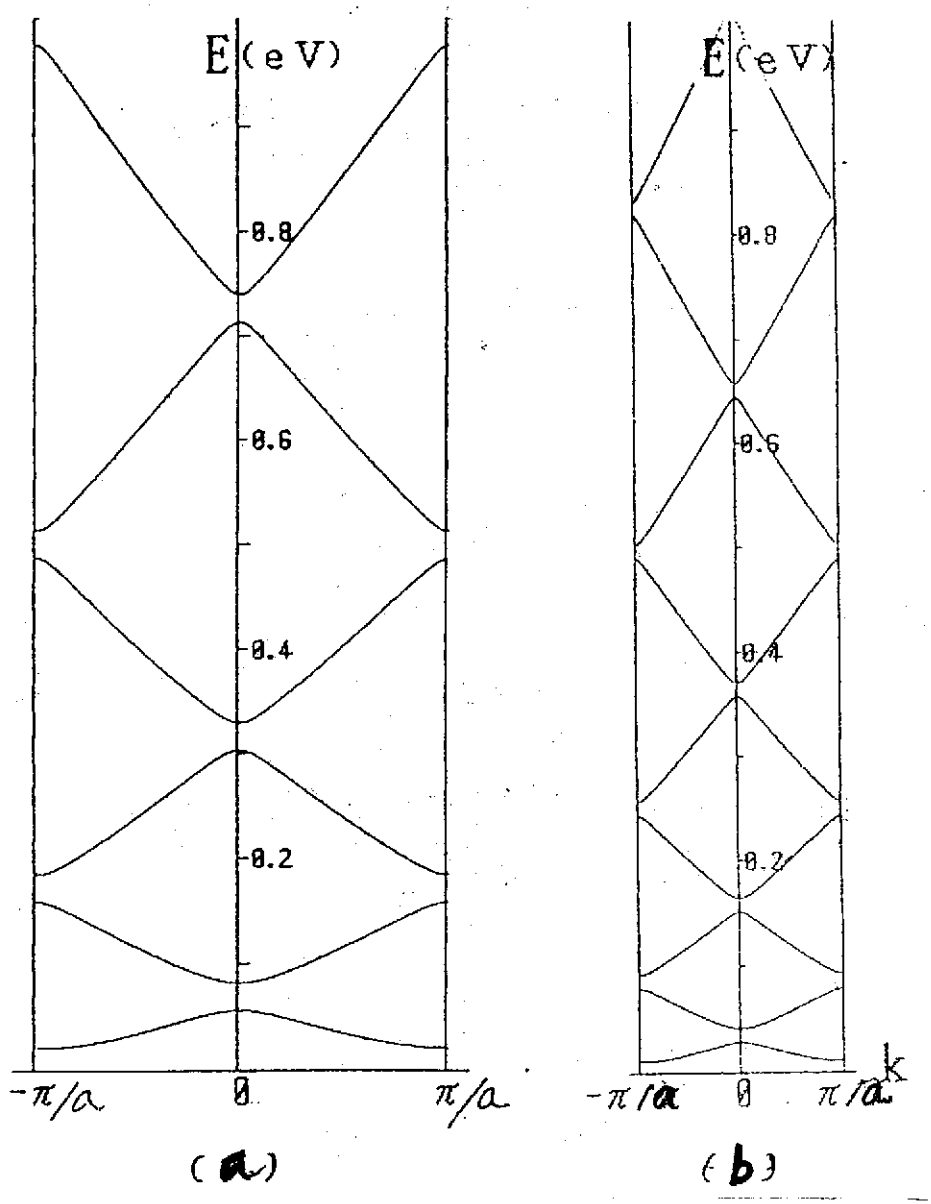

Neutron conduction bands are those above zero energy usually occupied by cold and thermal neutrons used in basic researches of basic properties of neutrons in solids and in neutron diffraction.

5-2. Neutron Valence Bands

H. Kozima, "Excited States of Nucleons in a Nucleus and Cold Fusion Phenomenon in Transition-Metal Hydrides and Deuterides" *Proc. ICCF9* (to be published);

H. Kozima, "Anomalous Nuclear Reactions and Atomic Processes in Transition-Metal Hydrides and Deuterides" *J. New Energy* **6-3** (2002) (to be published).

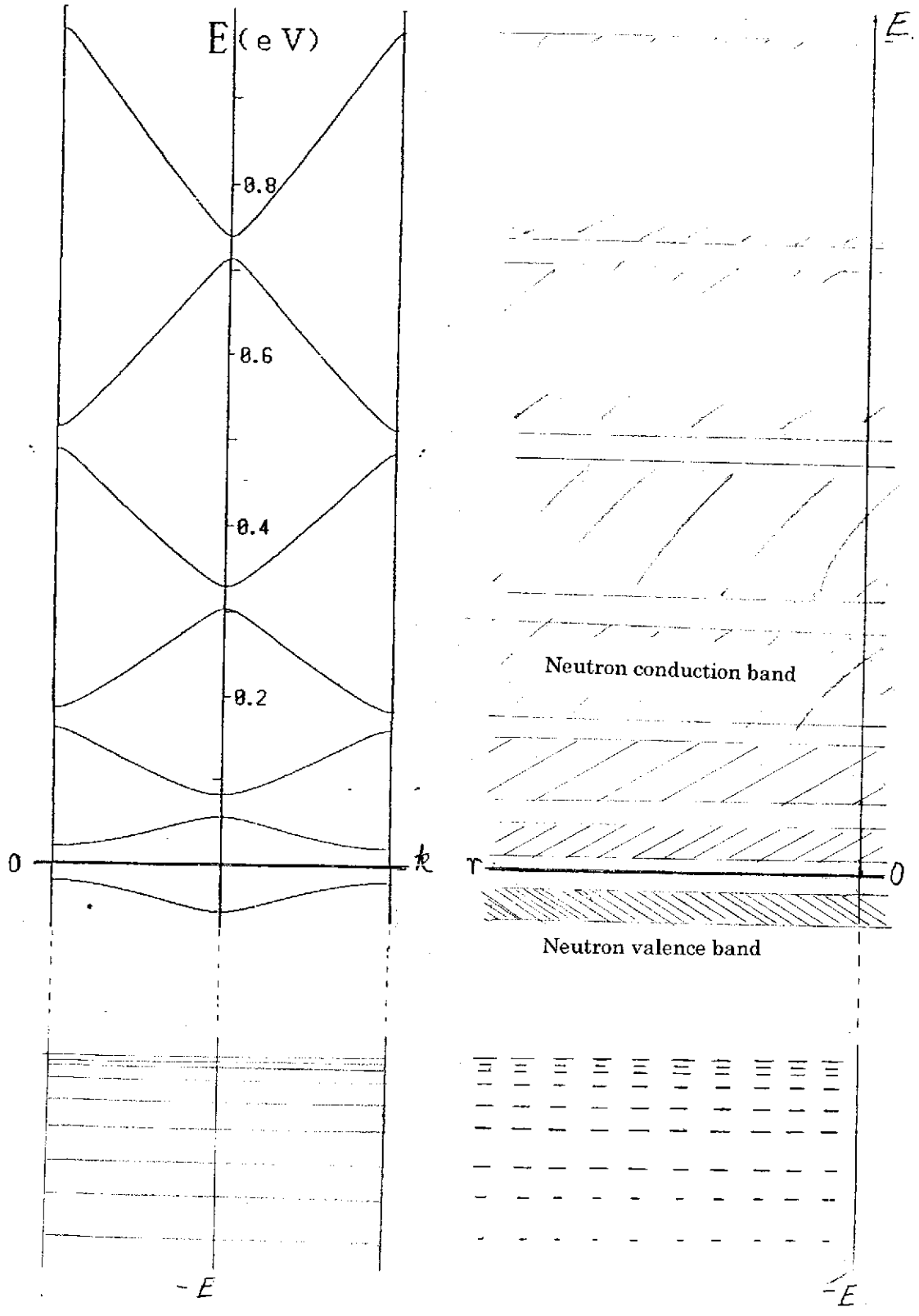

Neutron valence bands are neutron bands consisted of excited neutron levels in lattice nuclei at about zero energy (in the scale where the origin of the energy scale corresponds to the state at which a neutron is at rest outside the nucleus) mediated by occluded hydrogen isotopes in interstitial sites.

Assuming existence of high-density levels of a neutron in a Pd nucleus at near zero level in PdH or PdD, we can show existence of interaction between neutrons in these levels mediatied by hyrogen isotopes in intersticial sites. The interaction (let call it "the super-nuclear interaction") results in formation of a band structure in energy levels of neutrons in solids with energies a little below zero.

5-3. Local Coherence of Neutron Bloch Waves at Boundary

H. Kozima, K. Arai, M. Fujii, H. Kudoh, K. Yoshimoto and K. Kaki, "Nuclear Reactions in Surface Layers of Deuterium-Loaded Solids" *Fusion Technol.* **36**, 337 (1999).

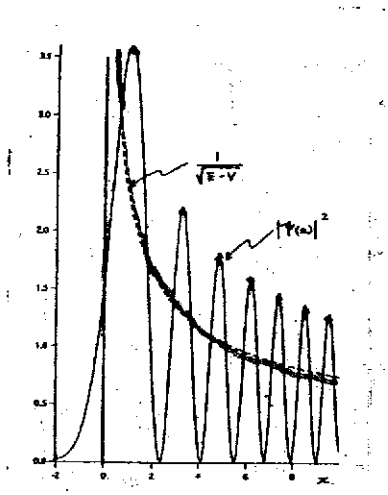

$y = a \sum \sin 2\pi(k_i x + \alpha_i)$ $(a = 1,\ \alpha_i = 0,\ k_i = 1.000,\ 1.005,\ \cdots\ 1.050)$

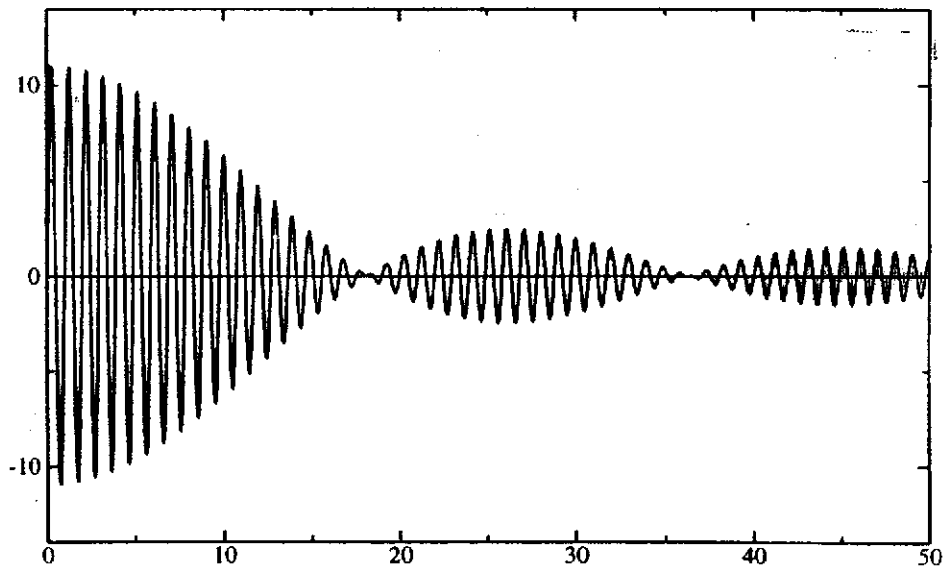

Bloch waves reflected at a boundary show local coherence when they have almost the same energy and somewhat different wave number vectors as we can understand clearly in the figures shown in the previous page.

5-4. Neutron Drops - Clusters of (A-ZNeutrons and (Z) Protons in CF Matter

H. Kozima, "Neutron Drop: Condensation of Neutrons in Metal Hydrides and Deuterides", *Fusion Technol.* **37**, 253 (2000).

H. Kozima, "The Cold Fusion Phenomenon and Physics of Neutrons in Solids" *Conference Proceedings* **70**(ICCF8), 449 (2000).

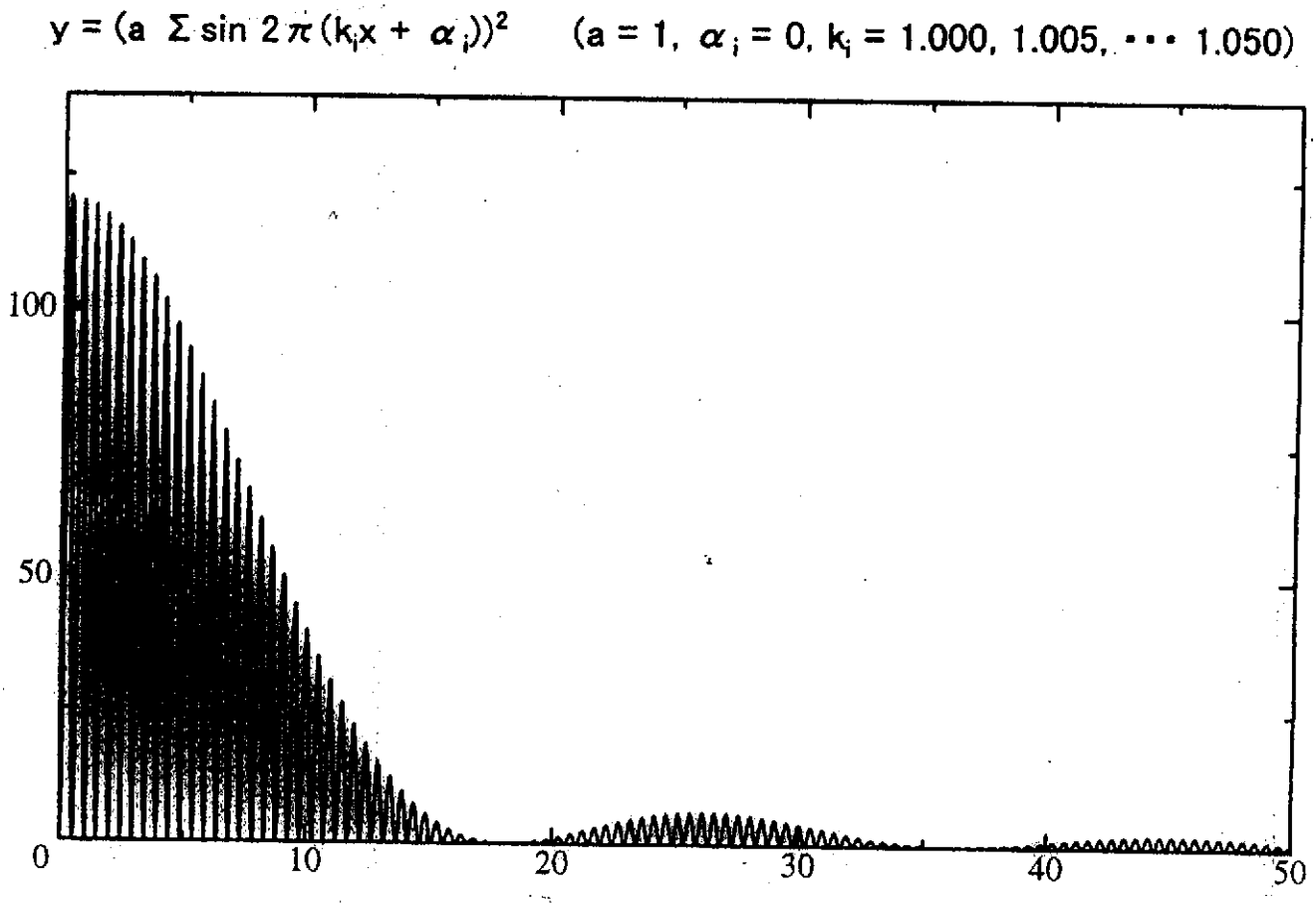

Neutron drops ${}^{A}_{Z}\Delta$ (${}^{A}_{Z}\Delta \equiv$ ((A-Z)n, Zp, Ze) (A $\gg$ Z) in thin neutron background) are formed when the density of neutrons become very high as 10^{30} cm^{-3} due to the local coherence of Bloch waves in the boundary region.

5-5. Analogy to Neutron Star Matter

J.W. Negele and D. Vautherin, "Neutron Star Matter at Sub-nuclear Densities" *Nuclear Physics* **A207**, 298 (1973).

Table 6: The theoretical and extrapolated to $n_G = 1 \times 10^{30}$ cm^{-3} values of the lattice constant a of Coulomb lattice and the proton-to-neutron ratio $\bar{x}$ in the neutron drops ${}^{A}_{Z}\Delta$(n-p clusters) as functions of n_G, where n_G is the density of the neutron gas surrounding the neutron drops in the Coulomb lattice. For reference, a and $\bar{x}$ for the lattice of Pd metal (composed of ${}^{110}_{46}$Pd) is added.

Density n_G(cm^{-3})	5×10^{37}	5×10^{36}	5×10^{35}	4×10^{34}	1×10^{30}	(Pd metal)
Estimated a (Å)	4×10^{-4}	7×10^{-4}	8.7×10^{-4}	1.1×10^{-3}	2×10^{-3}	$a_{Pd} = 2.5$
Estimated $\bar{x}$	0.28	0.45	0.53	0.53	0.7	$\bar{x}_{Pd} = 0.72$

Simple extrapolation of the result obtained in neutron star matter problem to lower density situations gives an interesting feature of transition-metal hydrides and deuterides in boundary layers where lattice nuclei are distributed in the Coulomb lattice of the neutron drops.

Fig.3 of J.W. Negele and D. Vautherin, Proton and neutron density distribution

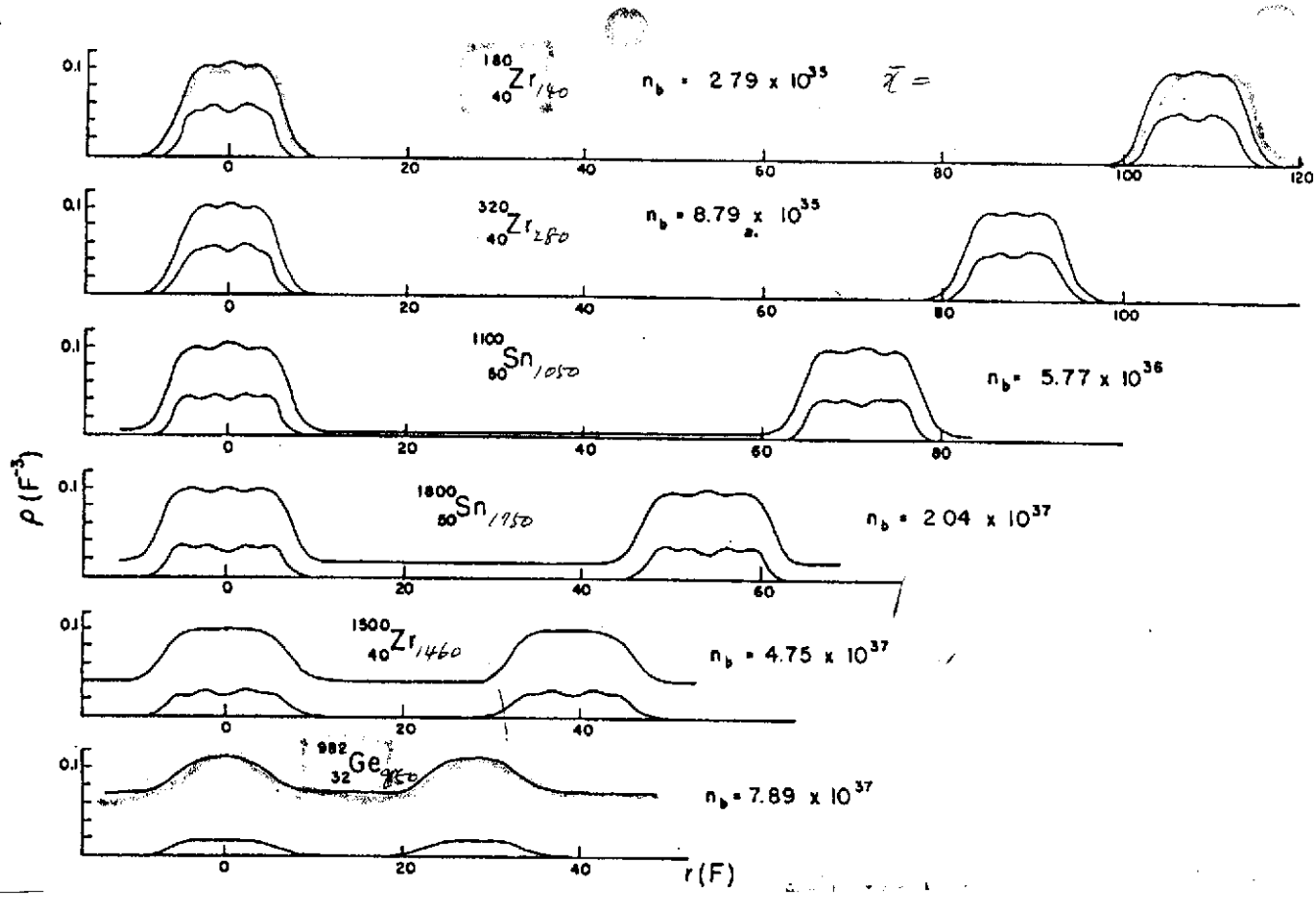

6. Nuclear Reactions in Solids

6-1. Interaction between Neutron Drops and Lattice Nuclei – Decay-Time Shortening, Gammaless Nuclear Reactions and Fission-Barrier Decrease

6-2. Nuclear Transmutation by Decay NT_D

6-3. Nuclear Transmutation by Fission NT_F

6-4. Nuclear Transmutation by Absorption NT_A

6-5. Decay Time Shortening in CFP

Interaction of neutron drops ${}^{A}_{Z}\Delta$ and lattice nuclei ${}^{A'}_{Z'}\mathrm{M}$ results in various characteristic nuclear reactions in solids completely different from those in free space.

6-1. Interaction between Neutron Drops and Lattice Nuclei – Decay-Time Shortening and Fission-Barrier Decrease

There appear several channels to dissipate the energy of an excited nuclide interacting with neutron drops that are absent when the nuclide is isolated in free space.

$$
\begin{aligned}
{}^{A}_{Z}\mathrm{M} + {}^{A'}_{Z'}\Delta &\rightarrow {}^{A''}_{Z''}\mathrm{M}'^{*} + {}^{A'''}_{Z'''}\Delta \\
{}^{A}_{Z}\mathrm{M}^{*} + {}^{A'}_{Z'}\Delta &\rightarrow {}^{A-b}_{Z-a}\mathrm{M}' + {}^{A'}_{Z'}\Delta^{*}
\end{aligned}
$$

where A + A′= A″+ A‴, Z + Z′= Z″+ Z‴should be satisfied. The neutron drop ${}^{A'''}_{Z'''}\Delta$ is turned into ${}^{A'}_{Z'}\Delta$ through the interaction with a thin neutron gas in the background. The new nuclide ${}^{A''}_{Z''}\mathrm{M}'^{*}$ stabilizes 1) by fission (fission-barrier decrease) or decay (decay-time shortening) generating several new nuclides or 2) by losing energy to be a stable nuclides ${}^{A''}_{Z''}\mathrm{M}'$.

This might be reasons of characteristic nuclear reactions in solids, i.e.
a) gammaless de-excitation of nuclides in excited states,
b) decay-time shortening of radioactive nuclides,
c) fission-barrier decrease of neutron-excess nuclides,
d) formation of largely nucleon-number shifted nuclides,
and so forth.

6-2. Nuclear Transmutation by Decay NT_D

$$n + {}^{6}_{3}\mathrm{Li} = {}^{4}_{2}\mathrm{He}\ (2.1\ \mathrm{MeV}) + t\ (2.7\ \mathrm{MeV}).$$

$$\begin{aligned}
{}^{40}_{19}\mathrm{K} &\rightarrow {}^{40}_{20}\mathrm{Ca} + e^- + \bar{\nu}_e, \quad (\tau \sim 10^9 \mathrm{y}) \\
{}^{109}_{46}\mathrm{Pd} &\rightarrow {}^{109}_{47}\mathrm{Ag} + e^- + \bar{\nu}_e, \quad (\tau \sim 10^6 \mathrm{y}) \\
{}^{238}_{92}\mathrm{U} &\rightarrow {}^{234}_{90}\mathrm{Th} + \alpha. \quad (\tau = 4.5 \times 10^9 \mathrm{y})
\end{aligned}$$

To understand appearence of nuclides ${}^{40}_{20}\mathrm{Ca}$, ${}^{109}_{47}\mathrm{Ag}$ and ${}^{234}_{90}\mathrm{Th}$ with enough amount, it is necessary to consider decay time shortening of these nuclides ${}^{40}_{20}\mathrm{K}$, ${}^{109}_{47}\mathrm{Pd}$ and ${}^{238}_{90}\mathrm{U}$, respectively.

6-3. Nuclear Transmutation by Fission NT_F

Data by Miley et al.

$${}^{A}_{46}\mathrm{Pd} + {}^{A'}_{Z'}\Delta \rightarrow {}^{A+a}_{46}\mathrm{Pd}^* + {}^{A'-a}_{Z'}\Delta$$

$$\begin{aligned}
{}^{A+a}_{46}\mathrm{Pd}^* &= {}^{A'}_{13}\mathrm{Al} + {}^{A''}_{33}\mathrm{M}, \\
&= {}^{A'}_{29}\mathrm{Cu} + {}^{A''}_{17}\mathrm{Cl}, \\
&= {}^{A'}_{23}\mathrm{V} + {}^{A''}_{23}\mathrm{V}, \\
&= {}^{A'}_{28}\mathrm{Ni} + {}^{A''}_{18}\mathrm{Ar}, \\
&= {}^{A'}_{26}\mathrm{Fe} + {}^{A''}_{20}\mathrm{Ca}, \\
&= {}^{A'}_{27}\mathrm{Co} + {}^{A''}_{19}\mathrm{K}, \\
&= {}^{A'}_{24}\mathrm{Cr} + {}^{A''}_{22}\mathrm{Ti}, \\
&= {}^{A'}_{30}\mathrm{Zn} + {}^{A''}_{16}\mathrm{S}, \\
&= {}^{A+1}_{47}\mathrm{Ag} + e^- + \bar{\nu}_e.
\end{aligned}$$

To understand appearence of nuclides on the right sides of these reaction formuli with enough amount, it is necessary to consider drastic decrease of fission barrier of these nuclides ${}^{A+a}_{46}\mathrm{Pd}$ or simultaneous absorption of many nucleus (a $\gg$ 1).

6-4. Nuclear Transmutation by Absorption NT_A

$$
\begin{aligned}
{}^{A}_{22}\mathrm{Ti} &\rightarrow {}^{A+a}_{24}\mathrm{Cr}, && \text{(Dash } et\ al.,\ \delta Z = 2) \\
{}^{A}_{38}\mathrm{Sr} &\rightarrow {}^{A+a}_{42}\mathrm{Mo}, && \text{(Iwamura } et\ al.,\ \delta Z = 4) \\
{}^{A}_{46}\mathrm{Pd} &\rightarrow {}^{A+a}_{48}\mathrm{Cd}, && \text{(Dash } et\ al.,\ \delta Z = 2) \\
{}^{A}_{46}\mathrm{Pd} &\rightarrow {}^{A+a}_{56}\mathrm{Ba}, && \text{(Yamada } et\ al.,\ \delta Z = 10) \\
{}^{A}_{46}\mathrm{Pd} &\rightarrow {}^{A+a}_{82}\mathrm{Pb}, && \text{(Yamada } et\ al.,\ \delta Z = 36) \\
{}^{A}_{55}\mathrm{Cs} &\rightarrow {}^{A+a}_{59}\mathrm{Pr}. && \text{(Iwamura } et\ al.,\ \delta Z = 4)
\end{aligned}
$$

To understand appearence of nuclides on the right sides of these reaction formuli with enough amount, it is necessary to consider drastic increase of mass and proton numbers in these nuclides ${}^{A}_{22}\mathrm{Ti}$, ${}^{A}_{38}\mathrm{Sr}$, ${}^{A}_{46}\mathrm{Pd}$, ${}^{A}_{55}\mathrm{Cs}$ without strong emission of radiation. Such a possibility is only conceivable in a situation where neutron drops in a thin neutron background interact with lattice neuclei and minor nuclei in the boundary layers.

6-5. Decay Time Shortening in CFP

Data by J. Dash et al.

Table 7: Alpha Radiation after Exposure of Uranium Samples to Hydrogen Isotope Plasmas(/Electroplated on Ni Cathodes)

(^{238}U + ^{235}U) Sample	Cntrl. I (^{238}U)	H1	H2	D1	D2	Cntrl. II (U_3O_8)	HD
Irradiation(/electrolysis) Time (h)	0	43	18	100	550	0	29.4
α (Counts/2h/gU(/100m/14.5mgU))	25160	59358	55994	57019	115267	380	670
α (Normalized Counts)	1	2.36	2.23	2.27	4.58	1	1.76
Inverse Normalized Counts	1	0.424	0.448	0.441	0.218	1	0.57

Summarized data showing decay time shortening and gammaless nuclear reactions.

Table 8: Alpha and Beta Radiations and Gammaless Reactions in Cold Fusion Phenomenon

U Sample	^{238}U	H1	H2	D1	D2	^{40}K	^{40}K[1]	^{107}Pd	^{107}Pd[2]	^{3}H*	^{3}H[3]
Decay mode	α	α	α	α	α	β	β	β	β	γ	n-^{3}H int.
$\tau(10^9$ y)	6.45	2.73	2.89	2.84	1.41	1		10^{-3}		10^{-19}	~ 0
τ_0/τ[*]	1	0.424	0.448	0.441	0.218	1	10^{-7}	1	10^{-11}	1	0
$\eta \equiv (\tau/\tau_0)$	1	2.36	2.23	2.27	4.58	1	10^{7}	1	10^{11}	1	$\geq 10^{20}$
n_n (10^8cm^{-3})		($\sim$ 1)	($\sim$ 1)	($\sim$ 1)	($\sim$ 1)		5.3×10^2		9×10^2		7×10^{-2}
$\eta/n_n(10^{-8}$cm^3)		(2.4)	(2.2)	(2.3)	(4.6)		5.3×10^5		10^8		$\geq 10^{21}$

) $\tau_0 \equiv 6.45 \times 10^9$ y (^{238}U), 10^9 y (^{40}K), 10^6 y (^{107}Pd), or 10^{-12} s (^{3}H).

1) ^{40}Ca detection. R.T. Bush, "A Light Water Excess Heat Reaction suggests that 'Cold Fusion' may be 'Alkali-Hydrogen Fusion' " *Fusion Technol.* **22**, 301 (1992).

2) ^{107}Ag detection. I.B. Savvatimova, Y.R. Kucherov and A.B. Karabut, "Cathode Material Change after Deuterium Glow Discharge Experiment", *Trans. Fusion Technol. (Proc. ICCF4)* **26**, 389 (1994).

3) ^{3}H detection. An example of the "gammaless nuclear reactions" widely noticed in the cold fusion phenomenon (CFP). The first observation of convincing tritium production is reported by N.J.C. Packham, K.L. Wolf, J.C. Wass, R.C. Kainthla and J.O'M. Bockris, "Production of Tritium from D_2O Electrolysis at a Palladium Cathode", *J. Electroanal. Chem.* **270**, 451 (1989).

Average decay time in the third low of Table 8 for H1, H2, D1 and D2 were calculated with an assumption the decay time shortening occurs homogeniously over the sample. Usually, nuclear reactions in CFP are localized at some regions with dimensions of about several μm in boundary layers with widths about several μm, the shortening in these region corresponding to the observed counts of the alpha decay given in Table 7 (third low) should be several orders of magnitude larger than given in the fifth low of Table 8.

7. Possible Applications

7-1. Production of Nuclides by NT

7-2. Remediation of Radiaoctive Nuclides by NT

7-3. Production of Large Nucleon Number Nuclides by NT_A

7-4. Liberation of Nuclear Energy

The physics of CFP summarized in the previous sections make possible to figure out possible applications of CFP for energy production, waste transmutation and production of necessary rare elements.

Problems in application of CFP

Because of the nuclear reactions accompanied with CFP, the subtle structure in materials enabling CFP are necessarily fragile and nuclides for the reactions are consumed. Therefore, it should be necessary to fabricate replaceable elements for the cold fusion apparatus. Anyway, it is definitely necessary to know physics of CFP more correctly and precisely for better utilization of CFP for applications.